Journal of the Korean Nuclear Society
Volume 32, Number 2, pp.142~156, April 2000

Interfacial Condensation Heat Transfer for Countercurrent Steam-Water Stratified Flow in a Circular Pipe

In-Cheol Chu and Moon Ki Chung
Korea Atomic Energy Research Institute
150 Dukjin-dong Yusong-gu, Taejon 305-353, Korea
chuic@kaeri.re.kr

Seon-Oh Yu and Moon-Hyun Chun
Korea Advanced Institute of Science and Technology
373-1, Kusong-dong, Yusong-gu, Taejon, 305-701, Korea

(Received August 2, 1999)

Abstract

An experimental study of steam condensation on a subcooled thick water layer (0.018 ~ 0.032 m) in a countercurrent stratified flow has been performed using a nearly horizontal circular pipe. A total of 103 average interfacial condensation heat transfer coefficients were obtained and parametric effects of steam and water flow rates and the degree of subcooling on condensation heat transfer were examined. The measured local temperature and velocity distributions in the thick water layer revealed that there was a thermal stratification due to the lack of full turbulent thermal mixing in the lower region of the water layer. Two empirical Nusselt number correlations, one in terms of average steam and water Reynolds numbers, and the water Prandtl number, and the other in terms of the Jakob number in place of the Prandtl number, which agree with most of the data within ± 25 %, were developed based on the bulk flow properties. Comparisons of the present data with existing correlations showed that the present data were significantly lower than the values predicted by existing correlations.

Key Words : interfacial condensation, thick water layer, temperature profile of water layer, horizontal circular pipe, countercurrent flow

1. Introduction

The modeling of direct-contact condensation heat transfer in a countercurrent steam-water stratified flow is of particular importance in the safety analysis of nuclear reactor systems. In the postulated loss-of-coolant-accident (LOCA) sequence of a PWR, emergency core cooling (ECC) water is injected into the reactor vessel through the cold legs to prevent overheating of the reactor core. The depressurization during the blow down phase of LOCA would result in

Table 1. Comparisons of Test Section Geometry, Experimental Conditions, and Heat Transfer Correlations for Direct Contact Condensation

No.	Author	Test Section Geometry & Test Conditions: a) Cross Section & b) Inclination (θ)(°)	Size (m): (Width × Height × Length)	a) Steam-Water Flow Direction b) System Pressure	a) Correlations for the Condensation Heat Transfer Coefficient b) Magnitude of Heat Transfer Coefficient
1	Linehan et al. (1970)	a) Rectangular b) Horizontal	~ 0.15 × 0.019 × 0.45	a) Concurrent b) Atmospheric	a) $St = \frac{Nu}{Re_f Pr_f} = 0.0073$ (A) b) h = 6 ~ 28 kW/m^2°C
2	Segev et al. (1981)	a) Rectangular b) 17°, 45° (degree from the horizontal)	0.152 × 0.051 × 1.066 (height is adjustable)	a) Countercurrent b) Atmospheric	a) For complete penetration and for both 17 and 45 deg inclinations: $Nu = 8.5\times10^{-4}Re_g^{0.25}Re_f^{0.85}Pr^{0.5}$ (B) b) h = 4 ~ 18 kW/m^2°C
3	Lim et al. (1984)	a) Rectangular b) Horizontal	0.3048 × 0.0635 × 1.601	a) Concurrent b) Atmospheric	a) For smooth interface (Average Nu): $\overline{Nu} = 0.534\overline{Re_g}^{0.58}\overline{Re_f}^{0.09}\overline{Pr}^{0.3}$ (C) For wavy interface (Average Nu): $\overline{Nu} = 0.0291\overline{Re_g}^{0.58}\overline{Re_f}^{0.42}\overline{Pr}^{0.3}$ (D) b) h = 1.3 ~ 20 kW/m^2°C
4	Kim et al. (1985)	a) Rectangular b) 4°, 30°, 33°, 87°	0.38 × (0.075, 0.038) × 1.27	a) Countercurrent b) Atmospheric	a) $Nu = 0.966\times10^{-3}Re_f^{0.98}Pr^{0.95}Fr^{0.8}$ (E) • The Froude number as a dimensionless gas velocity was found to be a better correlating paramter than the gas Reynolds number. b) h = 1 ~ 20 kW/m^2°C
5	Ruile (1995)	a) Rectangular b) Horizontal	0.079 × 0.066 × 1.20	a) Concurrent & Countercurrent b) Up to 5.5 MPa	• Compared his data with existing models. & No correlation is given.
6	Present Work	a) Circular b) Horizontal	I.D. = 0.084 Length = 2.20	a) Countercurrent b) Atmospheric	a) $\overline{Nu} = 7.96\times10^{-7}\overline{Re_f}^{1.31}\overline{Re_g}^{0.51}\overline{Pr}^{1.19}$ (F) $\overline{Nu} = 7.13\times10^{-9}\overline{Re_f}^{1.32}\overline{Re_g}^{0.53}\overline{Ja}^{1.21}$ (G) b) h = 0.240 ~ 1.145 kW/m^2°C

reverse core steam flow through the downcomer annulus, while the subcooled ECC water is brought into direct contact with escaping steam from the reactor core. Condensation heat transfer in direct-contact mode can also be encountered in a steam generator feedwater line and reflux condensers.

As summarized in Table 1, a number of experimental and analytical studies have been performed (Linehan et al., 1970; Segev et al., 1981; Lim et al., 1984; Kim et al., 1985; Ruile, 1995) to investigate the interfacial condensation heat transfer in stratified concurrent (Linehan et al., Lim et al.) and countercurrent (Segev et al., Kim et al., Ruile) steam-water flows over the past 30 years. The test section geometry and experimental conditions used by earlier workers that have been selected for comparison along with correlations obtained for direct contact condensation are shown in Table 1. Experimental parameter ranges and main conclusions of the earlier workers, on the other hand, are briefly outlined in Table 2 for reference. From Tables 1 and 2, following observations can

Table 2. Experimental Parameter Ranges and Main Conclusions of Various Workers

No.	Author	Test Parameters: Initial Conditions	Test Parameters: Water Layer Thickness (δ)(cm)	Dimensionless Numbers	Main Conclusions
1	Linehan et al. (1970)	1) $T_{f,in}$ = 21.1 ~ 93.3°C 2) $W_{f,in}$ = 0.045 ~ 0.051 3) $W_{g,in}$ = 0.011 ~ 0.017 (kg/s)	0.05 ~ 0.15cm (shallow)	$Re_{f,in}$ = 340 ~ 1,800 (film Reynolds No.) $Re_{g,in}$ = 14,000 ~ 17,500 Pr_f = 1.75 ~ 4.5	• The average Stanton number for 90 determinations was found to be 0.0073
2	Segev et al. (1981)	1) $W_{f,in}$ = 0.1; 0.21; 0.32; 0.43 2) $W_{g,in}$ = 0.025 ~ 0.105 (kg/s) 3) Inlet water temp. = 23, 77°C 4) Inclination angle: θ = 17, 45°		$Re_{f,in}$ = 2,330 ~ 10,030 $Re_{g,in}$ = 13,400 ~ 42,870	• For given conditions, h_i increases as film thickness decreases.
3	Lim et al. (1984)	1) $W_{f,in}$ = 0.2 ~ 1.45 2) $W_{g,in}$ = 0.04 ~ 0.16 (kg/s) 3) Inlet water temp. = 25, 50°C 4) Inlet water layer thickness = 0.95, 1.59, 2.22cm	At Inlet: 0.95cm; 1.59cm; 2.22cm At down-stream: 0.5 ~ 1.0cm (shallow)		• The heat transfer coeffs. increased with increasing steam flow rates and water flow rates.
4	Kim et al. (1985)	1) Inclination angle: θ = 4 ~ 87° 2) Aspect ratio (B/H): 5 and 10	0.1 ~ 0.7cm (shallow)	Re_f = 800 ~ 15,000 Re_g = 2,500 ~ 30,000	• For a given flow condition, the heat transfer coeff. increases as the water layer thickness decreases.
5	Ruile (1995)	1) Pressure: Up to 5.5 MPa 2) Inlet water temp. = 69.5 ~ 120.2°C 3) $W_{f,in}$ = 0.9 kg/s	~4cm (thick)	Re_f = 29,055 ~ 54,985 Re_g = 6,600 ~ 193,000	• Thick water layer prevents the full turbulent mixing & establishes thermal stratification.
6	Present Work	1) $W_{f,in}$ = 0.05 ~ 0.25 2) $W_{g,in}$ = 0.004 ~ 0.0085 (kg/s) 3) Inlet water temp. = 20, 40, 55°C	1.8 ~ 3.2cm (thick)	$\overline{Re}_f$ = 1,920 ~ 9,473 $\overline{Re}_g$ = 3,881 ~ 9,491 $\overline{Pr}$ = 2.5 ~ 5.6 $\overline{Ja}$ = 102 ~ 210	

be made:

(1) In all previous experimental studies, a rectangular channel and a very shallow water layer thickness have been used, as summarized in Table 2.

(2) The main test parameters were ① steam flow rate, ② water flow rate, ③ inlet subcooling, ④ inclination angle, ⑤ aspect ratio, and ⑥ system pressure (only in Ruile' s work).

(3) All the empirical correlations shown in Table 1 have a power-law relationship of the dimensionless flow properties. However, the coefficients of these correlations are inconsistent varying from one author to another.

(4) The dimensionless numbers used in the

Nusselt number correlations are slightly different from one author to another: ① Linehan et al. used Stanton number, ② both correlations of Segev et al. and Lim et al. include Reynolds numbers of steam and water and Prandtl number. However, Segev et al. used local parameters, whereas Lim et al. used average numbers. ③ Kim et al., on the other hand, used Froude number in place of the Reynolds number.

(5) The magnitude of measured condensation heat transfer coefficients varied from 1 kW/m^2 ℃ to 28 kW/m^2 ℃.

Most of the piping of a Nuclear Power Plant has a circular geometry rather than rectangular. Therefore, the flow geometry used in the existing works is not directly applicable to nuclear piping system. When the cross sectional area of a wide rectangular channel and that of a circular pipe are the same, the water layer of the circular channel will be much thicker than that of the wide rectangular channel for given flow rates of steam and water. In particular, when water layer thickness is increased, the characteristics of heat, mass and momentum transport, such as turbulent intensity and efficiency of turbulent mixing in the water layer, which play a dominant role in the interfacial condensation heat transfer, would be changed. Therefore, the difference in the flow geometry may result in the change of overall interfacial condensation heat transfer characteristics. According to the Ruile' s study (1995), the thick water layer (~ 40 mm) prevented full turbulent mixing and established thermal stratification. The limited turbulent mixing in the water layer, in turn, reduced the convective heat transfer mechanism as well as the interfacial heat and mass transfer property.

One of the flow channel configurations which suffers from lack of experimental data is the countercurrent flow of steam and a thick water layer in a circular pipe. The main objective of the present experimental study was to evaluate the condensation heat transfer of saturated steam in direct contact with the countercurrent flow of a subcooled thick water layer in a nearly horizontal circular pipe. The present study is also aimed at the determination of parametric effects of thick water layer, steam and water flow rates, and subcooling on the direct contact condensation phenomenon.

2. Experiments

A series of experiments were performed and a total of 103 data for the average interfacial condensation heat transfer coefficient have been obtained for various combinations of inlet water and steam flow rates and subcooling of the inlet water.

2.1. Experimental Apparatus

A schematic view of the present experimental apparatus is shown in Fig.1. The test facility was designed and constructed such that the condensation rates of steam along the circular channel could be measured while saturated steam and subcooled water flow in opposite direction. The test apparatus consists of (1) a test section, (2) steam and water supply system, (3) associated piping, and (4) data acquisition system. The test section, on the other hand, is slightly inclined (0.2° from the water inlet) and consists of four transparent tempered glass pipes which are connected in series by flanges. A traversable pitot tube (O.D. of 3.0mm) and a thermocouple (O.D. of 0.5mm) are installed at the bottom of each flange located at four different axial positions, as depicted in Fig.2. The total length and inside diameter of the horizontal channel are 2.2 m and 0.084 m, respectively. The steam, which is

Table 3. Test Matrix of the Present Experiments

	Water Inlet Temp.(℃)	Water Flow Rate (kg/s)	Steam Flow Rate (kg/s)	Re_f	Re_g	No. of Data
1st Exp.	20, 40, 50	0.13, 019, 025 0.010	0.006, 0.007, 0.008	3,908~9,473; 14,353*	883~9,164	32
2nd Exp.	20	0.05~0.25 (7cases)	0.0045~0.0085 (7cases)	1,920~7,294	4,552~9,492	36
	40	0.08~0.18 (4 case)	0.004~0.0065 (6case)	4,108~8,221	3,881~7,301	20
	55	0.08~0.15 (3 cases)	0.004~0.0065 (6 cases)	5,015~8,495	4,766~7,898	15
Total Number of Experimental Data						103

When the test section is 2° inclined

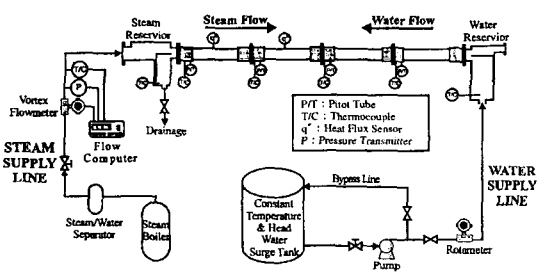

Fig. 1. Schematic Diagram of the Experimental Apparatus

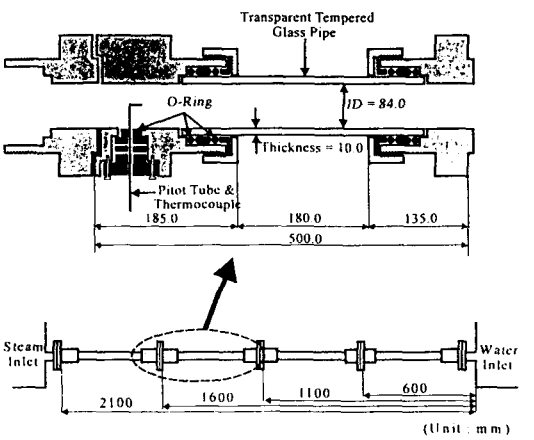

Fig. 2 Dimensions of the Test Section

supplied by a 200 kW electric steam boiler, passes through a steam-water separator, and a set of steam flow rate and thermal property measurement system before it flows into the test channel. The steam-water separator is used to ensure the supply of dry saturated or slightly superheated steam. The volumetric steam flow rate at the inlet of the test section is measured by a vortex flowmeter. The density of steam, on the other hand, is evaluated from the temperature and the pressure measured by a thermocouple and an absolute pressure transducer. A water surge tank (1.0 m^3) is used to provide a steady flow rate and the constant temperature of water that flows into the test section. The volumetric flow rate of water flowing into the test section is measured by a calibrated magnetic flowmeter and rotameter. The vortex flowmeter and magnetic flowmeter were calibrated at KRISS(Korea Research Institute of Standards and Science), and the pitot tubes were calibrated using a specially designed calibration loop.

2.2. Test Parameters and Test Procedure

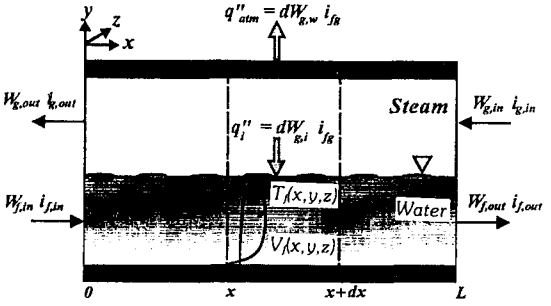

Fig. 3. Control Volume of the Countercurrent Steam-water Stratified Flow

The controllable test parameters were (1) the inlet flow rates of water and steam, and (2) the subcooling of the inlet water. A total of 103 runs were made for various combinations of inlet water and steam flow rates at three different inlet water temperatures of 20, 40, and 55 ℃ under atmospheric conditions, as summarized in Table 3. The range of Reynolds numbers for water and steam were 1,920 ~ 9,473 and 3,881 ~ 9,491, respectively. The Prandtl number and the Jakob number for water varied from 2.50 to 5.60 and from 102 to 210, respectively.

In the present work, the condensation rate of steam at the steam-water interface has been deduced from the measurement of the rate of increase in bulk water temperature due to steam condensation. To evaluate the rate of increase in bulk water temperature along the flow stream, radial (i.e., in y-direction as indicated in Fig. 3) distributions of velocity and temperature of the water at four axial positions along the test section were measured. A brief outline of the test procedure is as follows: (1) The water temperature in the surge tank was first brought to a predetermined value for each test run. The inlet flow rates of water and steam were then set at desired values using the pump controller and the valve, respectively. (2) When the desired steam and water flow rates have reached steady conditions, radial distributions of temperature and the velocity of water at four different axial positions along the test section (i.e., 0.6, 1.1, 1.6, and 2.1 m from the water inlet) are simultaneously measured by traversing the pitot tubes and thermocouples from the pipe surface to the steam-water interface (in the y-direction). The pitot tubes and thermocouples were attached to a digital vernier caliper-mounted traversing system such that both pitot tubes and thermocouples (whose tip was bent at 90°) could be raised vertically by an increment of 0.01 mm. All measurements, other than water film thickness, are recorded by the data acquisition system. (3) The water layer thickness (δ) at four axial positions is determined by visual observations and subcooling of the water measured by the thermocouples.

3. Methods of Analysis

An outline of the procedure to obtain the interfacial condensation heat transfer coefficient from the above measurement is as follows:

(1) Based on the local profiles of the measured temperature and velocity of water, the bulk water temperature and physical properties corresponding to bulk water temperature at the four axial positions are determined using following assumptions:
   ① The steam along the test section is at saturation conditions.
   ② The temperature and the velocity of water across the cross-section (in the z-direction) at each vertical position (in the y-direction) is uniform and has the 1/7 power velocity distribution, respectively.

It may be noted here that additional analyses showed that the velocity profile in the z-direction had not only a negligible effect on bulk water

temperature, but also the laminar flow velocity profile (instead of the 1/7 power velocity profile) did not change the bulk water temperature.

(2) The temperature of the bulk water is obtained by integrating the measured local temperature and velocity profiles over the area of water layer and using assumption ② given above as follows:

$$T_f(x)=\frac{\int \rho_f(x,y,z)T_f(x,y,z)V_f(x,y,z)dydz}{\int \rho_f(x,y,z)V_f(x,y,z)dydz} \quad (1)$$

Because of the difficulty of measuring velocity near the steam-water interface, the velocity of this region is evaluated by extrapolating the measured velocity profile with the assumption of no-slip at the interface.

(3) Using relations of the mass and energy conservation for the control volume shown in Fig.3, and the measured bulk water temperature, the local mass flow rate of water can be expressed as:

$$W_f(x)=\frac{W_{f,in}(i_g-i_{f,in})+\int_0^x q''_{atm}S_g dx}{i_g-i_f(x)} \quad (2)$$

The steam condensation rates at the wall of the test section and steam reservoir have been evaluated by direct measurement of the heat flux to the atmosphere using a micro-foil heat flux sensor. The results showed a wall condensation rate can be neglected in the actual calculation of the interfacial condensation heat transfer coefficient in the present work.

(4) Based on the mass and energy balance, the local interfacial condensation heat transfer coefficient at any location x from the water inlet can be expressed as:

$$h(x)=\frac{i_{fg}}{S_i(T_g-T_f)}\frac{dW_f}{dx} \quad (3)$$

(5) The channel-average heat transfer coefficient can now be obtained by integrating the local heat transfer coefficient (Eq. 3) over the total channel length $0<x<L=2.1$ m:

$$\bar{h}=\frac{1}{L}\int_0^L h dx$$

$$=\frac{C_{p,f}}{LS_i}\left\{(W_{f,in}-W_f(L))+W_{f,in}\left[1+\frac{C_{p,f}(T_g-T_{f,in})}{i_{fg}}\right]\ln\left[\frac{\frac{W_{f,in}}{i_{fg}}C_{p,f}(T_g-T_{f,in})}{W_{f,in}\left(1+\frac{C_{p,f}(T_g-T_{f,in})}{i_{fg}}\right)-W_f(L)}\right]\right\} \quad (4)$$

(6) In addition, definitions of dimensionless numbers used in the present work are as follows:

$$\overline{\mathrm{Nu}}=\frac{\overline{hD_{h,f}}}{\overline{k_f}},$$

$$\mathrm{Re}_f=\frac{\rho_f V_f D_{h,f}}{\mu_f},\quad \mathrm{Re}_g=\frac{\rho_g V_g D_{h,g}}{\mu_g},$$

$$\mathrm{Pr}=\frac{C_{p,f}\mu_f}{k_f},\quad \mathrm{Ja}=\frac{\rho_f C_{p,f}(T_g-T_f)}{\rho_g i_{fg}}, \quad (5)$$

$$D_{h,f}=\frac{4A_{p,f}}{S_i+S_f},\quad D_{h,g}=\frac{4A_{p,g}}{S_i+S_g}$$

The average Reynolds numbers, Prandtl number, and Jakob number are obtained by taking the arithmetic average of the measured values at four axial positions along the test section.

4. Experimental Results and Discussions

A total of 103 average interfacial condensation heat transfer coefficients have been obtained for various combinations of the following initial conditions: (1) inlet water flow rate, (2) inlet steam flow rate, and (3) degree of water subcooling. The ratio of the water layer thickness to the pipe diameter varied from 0.217 to 0.386 which was much greater than those of the earlier workers who used a wide rectangular channel.

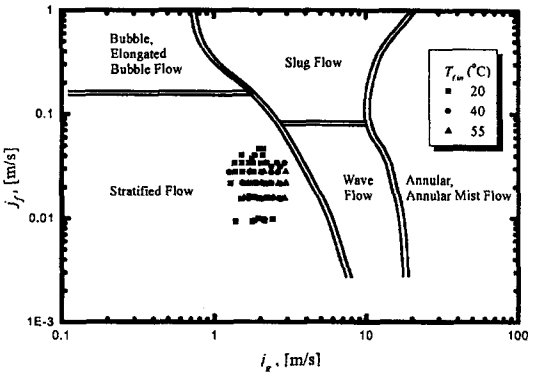

Fig. 4. Experimental Data Plotted in the Mandhane' s Flow Pattern map

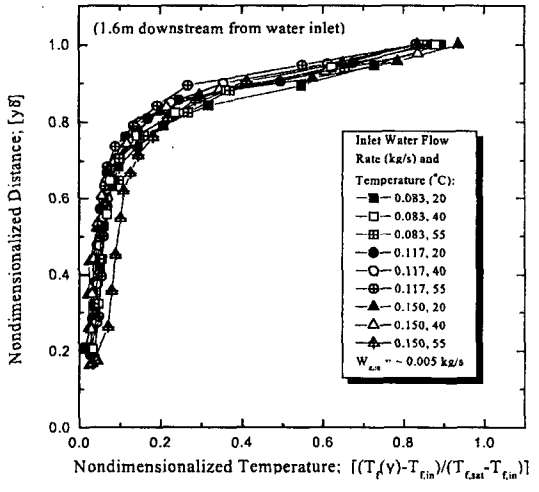

Fig. 5. Nondimensionalized Local Temperature Profiles of the Water Layer

4.1. Flow Regime

First, to examine the flow regimes of the present experimental conditions, present data are plotted on the Mandhane' s flow pattern map for gas-liquid flow in horizontal pipes (Mandhane et al., 1974) as shown in Fig.4. This figure shows that the present experimental conditions lie in the stratified regimes. Visual observations also showed that there was a smooth interface for most

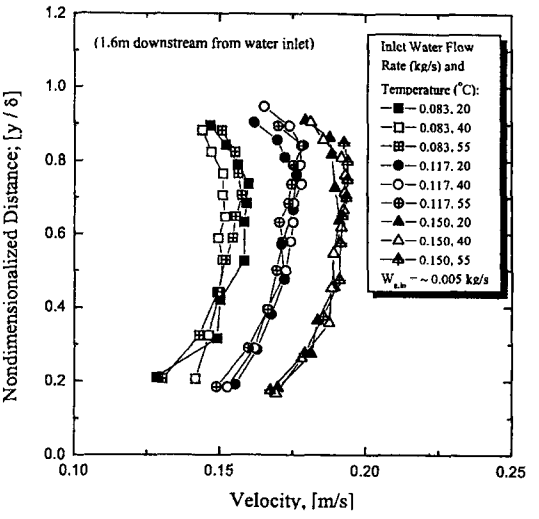

Fig. 6 Local Velocity Profiles of the Water Layer

cases and a small two-dimensional wavy interface for some cases throughout the experiments.

4.2. Profiles of Local Temperature and Velocity of Water

Figures 5 and 6 show typical profiles of local water temperature and local velocity measured at 1.6 m downstream from the water inlet for three inlet water temperatures of 20 ℃, 40 ℃, and 55 ℃. Figure 5 shows that local temperatures of the water layer close to the bottom (i.e., $y/\delta < 0.6$) is slightly higher than the inlet water temperature and remains fairly constant. In the higher water layer region (i.e., $y/\delta > 0.6$), however, the water layer temperature tends to rise sharply to the saturation temperature. Figure 6 also shows that the local velocity of the water layer reaches a high velocity region at around $y = \sim 0.01$ m and remains more or less constant (up to $y = \sim 0.015$ m), and then decreases at the region close to the steam-water interface ($y > \sim 0.015$ m). The curves shown in Figs. 5 and 6 imply that the thick water layer used in the present work (0.018-0.032 m)

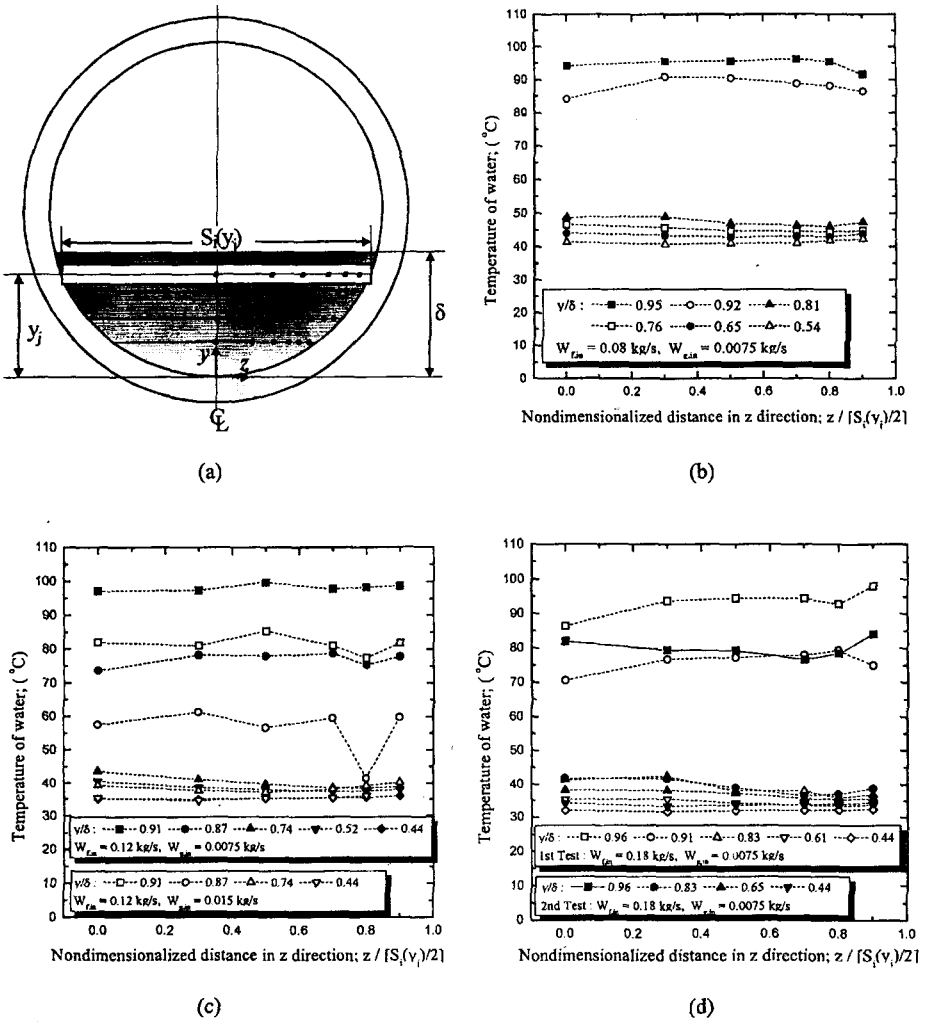

Fig. 7. Variations of Water Temperature in the z-direction at Different Levels of Water Layer (in the *y*-direction) for Various Flow Rates of Water(W_f) and Steam(W_g): (a) *y-z* Locations of Temperature Measurement, (b) W_f = 0.08 kg/s, W_g= 0.0075 kg/s, (c) W_f= 0.12 kg/s, W_g= 0.0075 and 0.015 kg/s, (d) W_f = 0.18 kg/s, W_g = 0.0075 kg/s

prevented the occurrence of full turbulent thermal mixing and established thermal stratification in the water layer. That is, effective turbulent thermal mixing was restricted within the narrow upper water layer (y/δ>~0.8) close to the steam-water interface region, and the turbulence generated by the interfacial shear did not propagate into the lower water layer region (y/δ<~0.8) below the steam-water interface. Therefore, the thermal resistance of water layer to the interfacial condensation heat transfer was fairly large.

In addition, for various flow rates of water and steam, variations of water temperature in the z-direction for different levels of water layer (i.e., in the *y*-direction as shown in Fig. 7(a)) were measured by traversing and rotating the

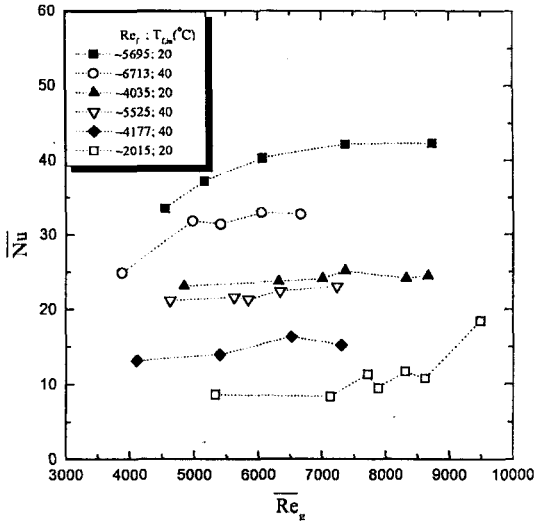

Fig. 8. Effects of Steam and Water Flow Rates on the Interfacial Condensation Heat Transfer ($\overline{Nu}$)

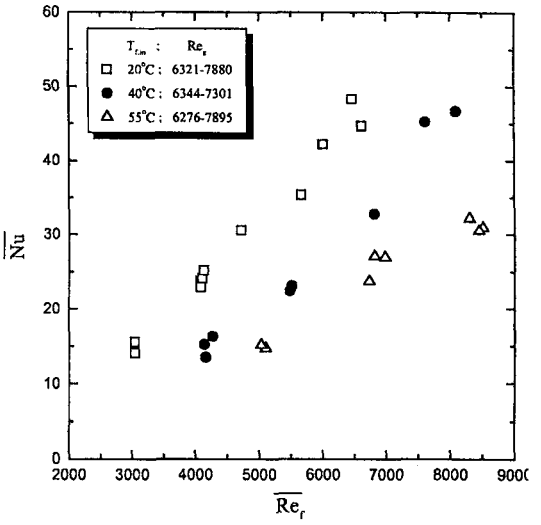

Fig. 9. Effect of the Subcooling of Water and Water Flow Rate on the Interfacial Condensation Heat Transfer ($\overline{Nu}$)

thermocouple installed at 1.6m downstream from the water inlet and the results are shown in Fig. 7(b) ~ (d). This figure shows that the temperature of water does not vary significantly in the z-direction.

4.3. Effects of Flow Rates of Steam and Water and Water Subcooling

As summarized in Table 1, the average interfacial condensation heat transfer coefficients obtained in the present work varied from 0.240 to 1.145 kW/m^2°C. In Fig.8, the average Nusselt number versus gas Reynolds number is shown for six different ranges of water Reynolds numbers and two given inlet water temperatures. The effects of water and steam flow rates on the average interfacial condensation heat transfer coefficient can be deduced from Figs.8 and 9. That is, for a given steam Reynolds number (or steam flow rate), the Nusselt number (or h) increases as the water Reynolds number (or water flow rate) is increased. Also, for a given water Reynolds number, the Nusselt number increases slightly when the steam Reynolds number is increased. However, the effect of the water flow rate is much greater than that of the steam flow rate. In this respect, it may be recalled here that the steam condensation rate depends on the activity of the liquid motion to transport thermal energy away from the interface into the water mainstream as already pointed out by earlier works (Lim et al., 1984). In the absence of complete turbulent mixing motion, it is the interface shear which enhances the convection. This explains the slight increase of the condensation heat transfer coefficient (or equivalently, Nusselt number) with higher steam Reynolds numbers. The increase in the condensation heat transfer coefficient with water flow rate, however, is mainly due to the following two factors: (1) at higher water flow rates, the water temperature increases slowly from the inlet value and therefore the temperature difference between the water layer and the steam remains relatively larger.

(2) an increase in the water flow rate may also increase initial turbulence in the water and therefore increase the condensation heat transfer. The effect of water subcooling on h was also studied by using three initial inlet water temperatures of 20 ℃, 40 ℃ and 55 ℃. As can be seen in Fig. 9, for about the same steam and water Reynolds numbers, the heat transfer coefficient increases as the bulk temperature of water is decreased (i.e., as the subcooling of water is increased).

4.4. Empirical Correlations for h

In an effort to correlate the 103 data obtained for the countercurrent steam-water flow in a nearly horizontal circular pipe, a channel average Nusselt number correlation has been developed in terms of the water and steam Reynolds numbers and water Prandtl numbers using a least-square fit method as follows:

$$\overline{Nu} = 7.96\times10^{-7}\,\overline{Re}_f^{1.31}\,\overline{Re}_g^{0.51}\,\overline{Pr}^{1.19} \qquad (6)$$

All the dimensionless numbers included in Eq.(6) are defined in terms of bulk flow properties as shown in Eq.(5).

The main purpose of developing an empirical average Nusselt number correlation in the form of a power-law relationship, in particular, is to follow the general practice used in turbulent forced convection and so it can be directly compared with other existing correlations. From the expression given in Eq.(6), following observations can be made: (1) the average Nusselt number (hence h) depends on both Reynolds numbers of water and steam. However, the effect of water Reynolds number (whose exponent is 1.31) is appreciably greater than that of the steam Reynolds number (whose exponent is only 0.51), and (2) the effect of water subcooling is included in Eq.(6) implicitly through the temperature dependent physical properties used in the definitions of Nu, Re_f, Re_g, and Pr.

However, another similar Nusselt number correlation has been developed that shows the effect of water subcooling more explicitly as follows:

$$\overline{Nu} = 7.13\times10^{-9}\,\overline{Re}_f^{1.32}\,\overline{Re}_g^{0.53}\,\overline{Ja}^{1.21} \qquad (7)$$

In Eq.(7), the Prandtl number used in Eq.(6) has been replaced by the Jakob number where the water subcooling is included in the definition as can be seen in Eq.(5). Since the steam temperature is essentially constant throughout the experiment, the Jakob number mainly depends on the bulk water temperature. Also, Jakob and Prandtl numbers decrease as the water temperature increases, and their sensitivities to water temperature are very similar. Therefore, there are no appreciable changes in the exponents of Pr and Ja numbers included in Eqs.(6) and (7), respectively.

4.5. Comparisons of Measured and Predicted Nusselt Numbers

A comparison of the measured Nusselt number with the calculated value from Eq.(7) is shown in Fig. 10. This figure shows that the agreement between the data and the correlation, Eq.(7), is within ±25% with a 92% confidence level. Equation (6) also agrees with the experimental data within ±25% with a 92% confidence level. Figures 11 and 12, on the other hand, show comparisons of the present experimental data with the existing correlations of Lim et al. (1984) and Kim and Bankoff (1983) developed for the smooth interface condition. To maintain consistency in the comparisons, the dimensionless numbers defined in Eq.(5) are converted to follow Lim's

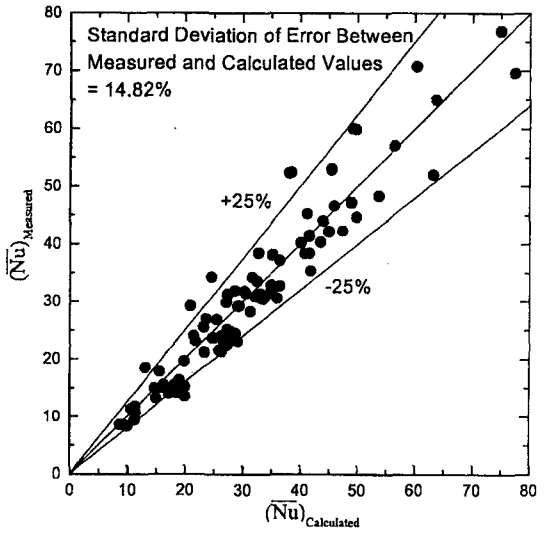

Fig. 10. Comparison of Measured Nusselt Number with the Calculated Value (Eq.7)

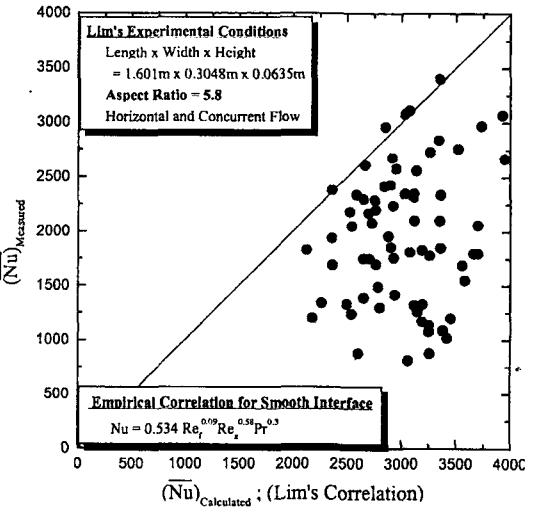

Fig. 12. Comparison of the Present Data with Lim' s Correlation

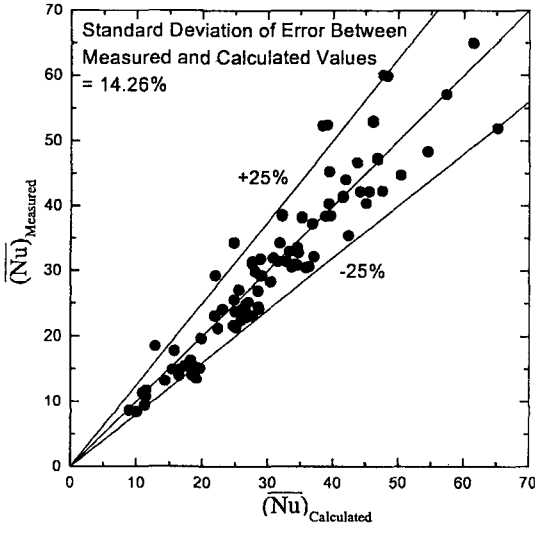

Fig. 11. Comparison of Measured Nusselt Number with the Calculated Value (Eq.6)

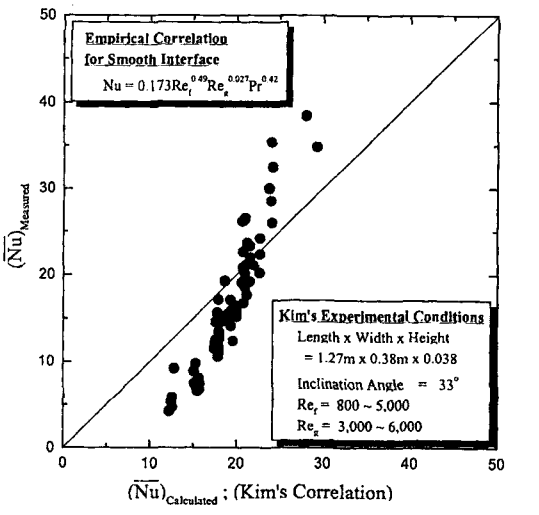

Fig. 13. Comparison of the Present Data with Kim' s Correlation

and Kim' s definitions. These figures show that there is a large disagreement between the present experimental data and the calculated Nu values of both correlations. In addition, both figures show that the heat transfer coefficients of the present experiments are considerably lower than those of the previous experiments when the water layer thickness in the definition of the Nusselt number is taken into account. The main reason for this discrepancy can be attributable to the differences

Table 4. Parameters and Estimated Uncertainties with 95% Confidence Interval

	Parameter	Bias Limit	Precision Limit
Independent Parameter	water layer thickness	1.0 mm	0.5 mm
	inlet water flow rate	3.0 %	0.7 %
	inlet steam flow rate	1.0 %	0.5 %
	local water velocity	5.0 %	0.8 %
	local water & steam temperature	2.2 ℃	0.1℃
Major Dependent Parameter	bulk water temperature	1.49 ~ 4.84 ℃	1.02~4.32 ℃
	water flow rate in test section	3.06 ~ 3.14 %	0.85 ~1.02 %
	steam flow rate in test section	5.5 ~ 19.9 %	2.6 ~ 7.7 %
	average heat transfer coefficient;	9.9 ~23.5 %	2.78 ~5.74 %
Uncertainty of average heat transfer coefficient; (R.M.S of Bias and Precision)		10.35 ~ 24.21 %	

in the water layer thickness and the geometry of the flow channel. That is, the present data are obtained from a circular pipe using relatively thick water layers (1.8 ~ 3.2 cm), whereas the correlations obtained by Lim et al. (1984) and Kim and Bankoff (1983) are based on a rectangular flow channel and a very shallow water layer thickness (0.1 ~ 0.4 cm, in the case of Kim and Bankoff). However, it is not possible to accurately quantify the dependency of the condensation heat transfer on the channel geometry and water layer thickness by comparing the present data with existing correlations, because there are other important differences in experimental conditions and ranges used by earlier works.

4.6. Uncertainty Analysis

Based on Eq. (4), the uncertainty in the present experimental result of heat transfer coefficients is given by the root mean square of a bias contribution and a precision (random) contribution to the uncertainty of heat transfer coefficient. Each of these two contributions can be evaluated separately in terms of the sensitivity coefficients of the reduced data to measured parameters (partial differential terms) and the measurement errors of the parameters using the uncertainty propagation equation of Kline and McClintock (1955). The uncertainty analysis has been performed in accordance with a 95 percent confidence interval and the detailed results are summarized in Table 4.

5. Conclusions

The interfacial condensation heat transfer for countercurrent steam-water stratified flow in a nearly horizontal circular pipe has been experimentally investigated. The main conclusions of the present work are as follows:

1. Condensation rates of atmospheric steam on a subcooled thick water layer (0.018 ~ 0.032 m) in a countercurrent horizontal circular channel were obtained by measuring the rate of increase

in bulk water temperature due to the condensation of steam and thereby average interfacial condensation heat transfer coefficients were deduced.

2. Results of the measurements of local temperature and velocity distributions in the thick water layer showed that there was a thermal stratification because the turbulent thermal mixing generated by the interfacial shear did not propagate into the lower water layer region but was restricted to the upper water layer region close to the steam-water interface.
3. The effects of the steam flow rates (0.004 ~ 0.0085 kg/s), water flow rates (0.05 ~ 0.25 kg/s), and inlet water temperature (20 ℃, 40 ℃, and 55 ℃) on condensation heat transfer were also examined.
4. Using a total of 103 average interfacial condensation heat transfer coefficient data obtained in the present work, two Nusselt number correlations, one [Eq.(6)] in terms of average steam and water Reynolds numbers, and the water Prandtl number, and the other [Eq.(7)] in terms of average steam and water Reynolds numbers, and the Jakob number, which agree with most of the data within ±25 % were developed.
5. Comparisons of the present experimental data with two existing correlations of Lim et al. (1984) and Kim and Bankoff (1983) showed that the present heat transfer coefficient data are considerably lower than the values calculated by two existing correlations. The main reason for this discrepancy can be attributable to the differences in water layer thickness and the geometry of the flow channel.

Nomenclature

A_p	cross-sectional flow area, (m^2)
C_p	specific heat, (J/kg℃)
D	inside diameter of circular channel, (m)
D_h	equivalent hydraulic diameter, (m)
Fr	Froude number = $\frac{V_g}{\sqrt{g(D-\delta)}}$
g	gravitational acceleration, (m/s^2)
h	local interfacial condensation heat transfer coefficient, (W/m^2℃)
$\overline{h}$	average interfacial condensation heat transfer coefficient, (W/m^2℃)
i	specific enthalpy, (J/kg)
i_{fg}	latent heat of condensation, (J/kg)
Ja	Jakob number
k	conductivity, (W/m℃)
L	channel length, (m)
Nu	Nusselt number
Pr	Prandtl number
q''_{atm}	heat flux to the atmosphere due to the steam condensation at the wall, (W/m^2)
q''_i	heat flux to the water layer due to the steam condensation at the interface, (W/m^2)
Re	Reynolds number
S	wall perimeter, (m)
S_i	interface perimeter, (m)
T	temperature, (℃)
$T_f(x)$	bulk water temperature, (℃)
V	velocity, (m/s)
W	mass flow rate, (kg/s)
x	axial distance from the water inlet, (m)
y	vertical distance from the pipe bottom, (m)
z	horizontal cross-stream distance from the pipe center line, (m)

Greek

δ	water layer thickness, (m)
θ	inclination angle, (degree; °)
μ	viscosity, (Ns/m^2)
ρ	density, (kg/m^3)

Subscript

f	water; water side
g	saturated steam; steam side
i	interface
in	inlet of water or steam
sat	saturated value

Superscript

—	average value

Acknowledgement

The authors gratefully acknowledge the financial support of Science & Technology Policy Institute (STEPI) provided for this work.

References

1. Kim, H. J. and Bankoff, S. G., "Local heat transfer coefficients for condensation in stratified countercurrent steam-water flows," J. Heat Transfer Trans. ASME, 105, 706-712 (1983).
2. Kim, H. J., Lee, S. C., and Bankoff, S. G., " Heat transfer and interfacial drag in countercurrent steam-water stratified flow," Int. J. Multiphase Flow, 11, 593-606 (1985).
3. Lim, I. S., Tankin, R. S., and Yuen, M. C., "Condensation measurement of horizontal cocurrent steam/water flow," J. Heat Transfer Trans. ASME, 106, 425-432 (1984).
4. Kline, S. J. and McClintock, F. A., "Describing uncertainties in single-sample experiments," Mechanical Engineering, 75, 3-8 (1953).
5. Linehan, J. H., Petrick, M., and, El-Wakil, M. M., "The condensation of a saturated vapor on a subcooled film during stratified flow," Chem. Eng. Prog. Symp. Series, 66, 11-20 (1970).
6. Mandhane, J. M., Gregory, G. A., and Aziz, K., "A flow pattern map for gas-liquid flow in horizontal pipes," Int. J. Multiphase Flow, 1, 537-553 (1974).
7. Moffat, R. J., "Describing uncertainties in experimental results," Experimental Thermal and Fluid Science, 1, 3-17 (1988).
8. Ruile, H., "Heat transfer by direct contact condensation in stratified two phase flow at high system pressure," Two-Phase Flow Modelling and Experimentation, 269-276 (1995).
9. Segev, A., Flanigan, L. J., Kurth, R. E., and Collier, R. P., "Experimental study of countercurrent steam condensation," J. Heat Transfer Trans. ASME, 103, 307-311 (1981).